Microchim Acta
DOI 10.1007/s00604-017-2420-z

ORIGINAL PAPER

Nanocomposites based on carbon nanotubes and redox-active polymers synthesized in a deep eutectic solvent as a new electrochemical sensing platform

Oana Hosu [1,2] · **Madalina M. Barsan** [1] · **Cecilia Cristea** [2] · **Robert Săndulescu** [2] · **Christopher M. A. Brett** [1]

Received: 21 February 2017 / Accepted: 10 July 2017

Abstract The redox polymer poly(methylene blue) was synthesized by electropolymerization in ethaline deep eutectic solvent (PMB_{DES}), and employed in a new nanostructured composite together with carbon nanotubes (CNT). The polymer was formed either before or after CNT deposition on glassy carbon electrodes (GCE) to obtain GCE/PMB_{DES}/CNT and GCE/CNT/PMB_{DES} modified electrodes, respectively. The morphology of the hybrid films was investigated by scanning electron microscopy, and their electrochemical performance by cyclic voltammetry and electrochemical impedance spectroscopy. The composite with the highest faradaic response and electronic conductivity was identified and applied as a platform for the determination of ascorbic acid by fixed potential amperometry at +0.2 V vs. Ag/AgCl, and acetaminophen by square wave voltammetry and differential pulse voltammetry at +0.67 V vs. Ag/AgCl. The limits of detection of the best sensor configurations are 1.7 μM for AA, and 1.6 μM for APAP, and respective electrochemical sensitivities are 2.2 $\mu A\ cm^{-2}\ \mu M^{-1}$ and 68.7 $\mu A\ cm^{-2} \mu M^{-1}$. The applicability of the electrochemical sensors was demonstrated by the successful quantification of both these key analytes in complex pharmaceutical formulations.

Keywords Ethaline deep eutectic solvent · Polymer-CNT hybrid · Electrochemical sensor · Ascorbic acid · Acetaminophen

Introduction

The combination of electroactive polymers with carbon nanotubes (CNT), has been an active area of research and, up to now, has been shown to be a successful combination in developing electrochemical sensors with improved analytical performance [1]. For the synthesis of electroactive polymer films, electropolymerisation from aqueous solution onto the electrode surface or onto the surface of carbon nanotubes, previously deposited on the electrode, is fast and is the most common method employed. In 2014, it was shown that the synthesis of conducting polymers in deep eutectic solvents offers the possibility to tailor the polymer structure and morphology, leading to polymers with improved electronic conductivity compared to those obtained in aqueous media [2, 3].

Among the electroactive polymers, the phenazine polymer poly(methylene blue) has been shown to have numerous applications in the (bio)sensing area, used either alone [4] or in combination with other conducting polymers, *e.g.* poly(1,2-ethylenedioxythiophene) (PEDOT) for determination of ascorbate, glucose and cholesterol [5, 6], or CNT for developing a sensor for acetaminophen and pyridoxine [1].

We have recently reported a new method for obtaining nanostructured films of poly(methylene blue) (PMB) in the deep eutectic solvent ethaline (PMB_{DES}), which is made from mixing choline chloride with ethylene glycol in the correct stoichiometric ratios [7]. It was shown that the nanostructured tailored polymer played an important role in the electrical properties of the films, and thence on the analytical

---

Electronic supplementary material The online version of this article (doi:10.1007/s00604-017-2420-z) contains supplementary material, which is available to authorized users.

✉ Christopher M. A. Brett
cbrett@ci.uc.pt

[1] Department of Chemistry, Faculty of Sciences and Technology, University of Coimbra, 3004-535 Coimbra, Portugal

[2] Department of Analytical Chemistry, Faculty of Pharmacy, “Iuliu Hațieganu” University of Medicine and Pharmacy, 400349 Cluj-Napoca, Romania

performance of the corresponding sensor, which was far superior to that using PMB synthesized in aqueous media (PMB_{aq}) [7].

This work focuses on the development of new composite electrode modifier materials comprising PMB_{DES} and CNT, in order to probe the added influence of CNT and any synergistic effects. The PMB_{DES} was deposited either on top or beneath the CNT layer on glassy carbon electrode (GCE) supports, and the morphologies of the resulting composites were analysed by scanning electron microscopy (SEM). Cyclic voltammetry (CV) was used together with electrochemical impedance spectroscopy (EIS) to analyse the electrochemical properties of the modified electrodes GCE/CNT/PMB_{DES} and GCE/PMB_{DES}/CNT. For comparison, modified electrodes with only one component, either CNT or PMB_{DES}, were also evaluated. The PMB_{DES}-CNT modified electrodes were then used as amperometric and voltammetric sensors for ascorbic acid and acetaminophen. Ascorbic acid (AA), vitamin C, is an electroactive compound usually added to foods and many pharmaceutical formulations due to its antioxidant and acidity regulator properties, and it was found that it can also be used as a potential treatment of infectious diseases and cancer [8]. New electrode platforms for more efficient detection of the antipyretic drug acetaminophen (APAP) are also being investigated [9]. AA and APAP were chosen to evaluate the electrocatalytic properties of the sensor by reducing the detection overvoltage and the increase in the sensor analytical signal. Both compounds were determined in several pharmaceutical formulations and the recovery factors were calculated.

Experimental

Reagents and solutions

All reagents were of analytical grade and were used without further purification. Millipore Milli-Q nanopure water (resistivity ≥ 18 MΩ cm) was used for the preparation of all solutions.

Methylene blue, choline chloride, ethylene glycol, L-ascorbic acid (AA), acetaminophen (APAP), potassium chloride, sodium hydroxide, and acetic, boric, hydrochloric and perchloric acids were purchased from Sigma Aldrich, Germany (www.sigmaaldrich.com). MWCNT were purchased from NanoLab, USA (www.nano-lab.com).

For the electrochemical characterization of the modified electrodes, the supporting electrolyte was 0.1 M KCl + 5 mM HCl solution (pH ≈ 4) and for the sensing studies the supporting electrolyte was 0.1 M KCl. All experiments were carried out at room temperature (25 ± 1 °C).

Instrumentation

Voltammetric experiments were performed in a three-electrode cell, containing the glassy carbon electrode (GCE-geometric area 0.00785 cm^2) as working electrode, a Pt wire counter electrode and an Ag/AgCl (3.0 M KCl) reference electrode, with a μ-Autolab potentiostat/galvanostat (Metrohm-Autolab, Netherlands, www.metrohm-autolab.com). Before each use, the surface of the GCE was cleaned with diamond spray on polishing paper (Kemet International, UK, www.kemet.co.uk) down to 1 μm particle size.

EIS experiments were carried by using a potentiostat/galvanostat/ZRA (Gamry Instruments, Reference 600, USA, www.gamry.com). A root mean square (rms) perturbation of 10 mV was applied over the frequency range 65 kHz – 0.1 Hz, with 10 frequency values per frequency decade. ZView 2.4 software (Scribner Associates, USA, www.scribner.com), was used to fit the spectra to equivalent electrical circuits.

The pH measurements were carried out with a CRISON 2001 μ pH-meter (Crison Instruments SA, Spain, www.crisoninstruments.com) at room temperature.

SEM (JEOL, JSM-5310, Japan, www.jeol.co.jp) was used to characterize the morphology of the different PMB_{DES} films deposited on carbon film electrodes.

Preparation of PMB_{DES} and CNT modified GCE

Multi-walled CNT were purified and functionalized in 3 M nitric acid, then washed and dried [10]. A dispersion of 1% CNT was prepared in chitosan solution (1.0% m/m chitosan dissolved in 1.0% v/v acetic acid). From this dispersion, 1 μL was dropped two times on the surface of GCE and allowed to dry.

Ethaline deep eutectic solvent was obtained by mixing choline chloride with ethylene glycol in a 1:2 M ratio and heating up to 60 °C. The polymerization solution contained 90% DES plus a 10% aqueous mixture of 0.1 M NaOH and $HClO_4$; the final monomer concentration in this mixture was 5 mM MB. The PMB_{DES} film was synthesized by cycling for 30 scans in the potential range from −0.6 to +1.1 V at 150 mV s^{-1} [7].

The polymer was deposited either on bare GCE to obtain GCE/PMB_{DES} on top of which CNT were drop cast resulting in the final architecture GCE/PMB_{DES}/CNT or on top of GCE/CNT to give GCE/CNT/PMB_{DES}.

Sample preparation

Pharmaceutical samples consisted of sachets containing both ascorbic acid and acetaminophen, which were dissolved in 50 mL distilled water. Sample aliquots of approximately twice the concentration of the standard were added for the standard addition method. The samples were: Aspirin Plus C® (240 mg ascorbic acid, 400 mg acetylsalicylic acid), FaringoHotDrink®

(250 mg ascorbic acid, 500 mg acetaminophen), Paramolan C® (200 mg ascorbic acid, 500 mg acetaminophen, 4 mg chlorpheniramine maleate), Coldrex Max Grip® (1 g acetaminophen, 10 mg phenylephrine hydrochloride, 40 mg ascorbic acid), and Theraflu Extra® (650 mg acetaminophen, 10 mg phenylephrine hydrochloride).

Results and discussion

The methodology of synthesising PMB polymer films with a new nanostructure and morphology, from DES, was applied in order to obtain hybrid composites of the polymer with CNT, on top of the GCE support. Two main types of composite were prepared, one with PMB on top of the CNT and the other with CNT on top of the electrosynthesised polymer film.

Preparation of GCE/CNT/PMB$_{DES}$ and GCE/PMB$_{DES}$/CNT

Cyclic voltammograms recorded during the polymerization of MB at GCE/CNT in DES are presented in Fig. 1a, with the inset showing MB polymerization at bare GCE, under the same experimental conditions. The polymerization profiles are different depending on the substrate. When polymerization occurs on GCE/CNT, the oxidation and reduction potentials of monomer and polymer are shifted towards less negative potentials, closer to 0.0 V vs. Ag/AgCl, with a more significant shift of the reduction potential. This corresponds to a more reversible redox process, CNT promoting faster electron transfer, as observed for formation of other phenazine films on CNT [1]. When MB is polymerized on the GCE substrate, there is a constant shift of the oxidation peak potential upon polymer formation with each cycle, and a decrease in monomer oxidation current, with an increase in polymer oxidation current. During MB polymerization on GCE/CNT, the monomer oxidation potential shifts during the first 3 cycles, then stays almost constant for the remaining 27 cycles, with a gradual increase in the oxidation peak current. The reduction wave is broader and less negative during PMB$_{DES}$ formation on GCE/CNT, the reduction peak potentials remaining the same during the polymerization as for PMB$_{DES}$ deposition on GCE.

The GCE/PMB$_{DES}$/CNT electrodes were made by first polymerizing MB on bare GCE followed by modification with a CNT layer.

The PMB$_{DES}$-CNT modified electrodes, in both configurations, were very stable, with less than 8% loss of initial current upon potential cycling for 100 cycles, whereas the PMB$_{DES}$ at GCE (without CNT) loses 10% of the initial current already after 30 scans [7], and 16% after 100 scans. Storage stability was evaluated by recording CVs after one month of storage in water at 4 °C and in air at ≈ 25 °C, giving 96% and 93% of the initial polymer redox peaks, when kept in water and in air, respectively. This high stability may be correlated with several

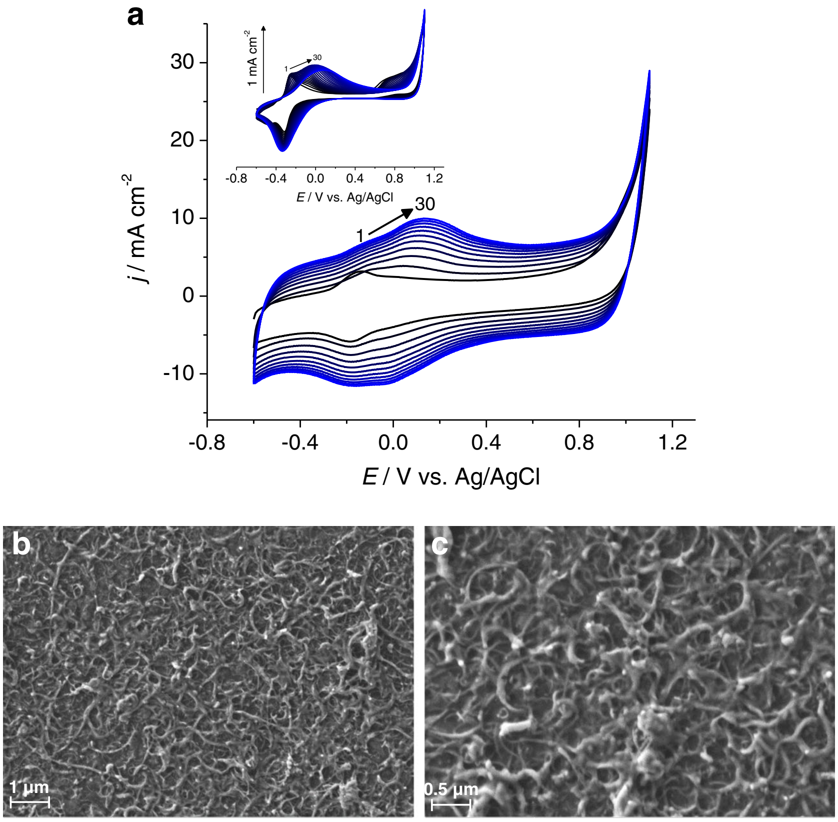

Fig. 1 **(a)** CVs recorded during polymerization of MB at GCE/CNT in a solution containing 5 mM MB in ethaline + 0.1 M NaOH + 0.1 M $HClO_4$ at 150 mV s^{-1} (every 3rd scan shown); inset - polymerization of MB at GCE; **(b)** and **(c)** are SEM images of GCE/CNT/PMB$_{DES}$ at different magnifications

interactions (*e.g.* electrostatic, π and hydrophobic interactions [1, 10]) occurring between CNT and PMB_{DES}.

Characterization of the GCE/PMB_{DES}/CNT and GCE/CNT/PMB_{DES} sensors

Scanning electron microscopy

SEM images were recorded at indium tin oxide (ITO) electrodes modified with CNT and PMB_{DES} with the same configurations as at GCE, *i.e.* ITO/PMB_{DES}/CNT and ITO/CNT/PMB_{DES}. SEM images of ITO/CNT and ITO/PMB_{DES} were also recorded for comparison (Fig. S1). With CNT covering the PMB_{DES}, the micrographs are very similar to those of ITO/CNT (Fig. S1a). The PMB_{DES} structure deposited on ITO reveals ultrafine cauliflower like nanoparticles (Fig. S1b), not visible when CNT covers the polymer. The morphology of CNT is considerably different after the deposition of PMB_{DES}, as seen in Figs. 1b and c, which reveal thicker tube-like structures, indicating that the polymer is deposited on the sidewalls of the CNTs. Also, the fact that the resulting composite is not as porous as the CNT network indicates that polymer is also formed between the CNT filaments, and that some of the CNT covered by PMB_{DES} may overlap. The diameter of the CNT covered by PMB_{DES} is 90 ± 15 nm. However, as seen in Fig. 1c, underneath the top layer of CNT/PMB_{DES}, some thinner filaments can be observed (d ≈ 50 nm) which indicates that the upper part of the layer of CNT is covered by thicker films of PMB_{DES}, this upper layer being more exposed to the monomer solution. More deeply inside the CNT network, less monomer is available, so that the film of PMB_{DES} covering the CNT is thinner, giving diameters only slightly higher than the unmodified CNT.

Cyclic voltammetry

CVs recorded in 0.1 M KCl + 5 mM HCl solution at GCE/CNT/PMB_{DES} and GCE/PMB_{DES}/CNT as well at the GCE modified with only one component, either CNT or PMB_{DES}, are shown in Fig. 2a. Anodic and cathodic peak currents are substantially higher for the PMB_{DES}-CNT hybrid films, compared to electrodes modified with only one component. Moreover, when CNT is on top of PMB_{DES}, the peak currents are almost a factor of two higher, probably due to a more open structure of the PMB_{DES}/CNT hybrid, which allows easier insertion/expulsion of the counter-ions involved in the redox processes. With PMB_{DES} on top of CNT, the CNT/PMB_{DES} composite, the CNT diameter is increased and part of the interstitial space is occupied by the PMB_{DES} film, as clearly seen in the SEM images in Fig. 1b and c, and which hinders diffusion inside the composite film.

The calculated capacitance values were 0.7, 12.5, 39.2 and 39.6 mF cm^{-2}, for GCE/PMB_{DES}, GCE/CNT, GCE/CNT/PMB_{DES} and GCDE/PMB_{DES}/CNT, respectively. Unlike for composites of CNT and polyphenazine films made in aqueous solutions, where the capacitive current contribution is attributed to CNT, the capacitive currents of the PMB_{DES}-CNT modified electrodes are considerably higher than that of GCE/CNT [1]. This is most probably related to the controlled nanoscale structure of the PMB films formed in DES, which allows much more charge to be stored in the film. It is interesting to observe that PMB_{DES}-CNT modified electrodes, in both architectures, exhibited similar capacitance values of ≈ 40 mF cm^{-2}, twice that of GCE/CNT.

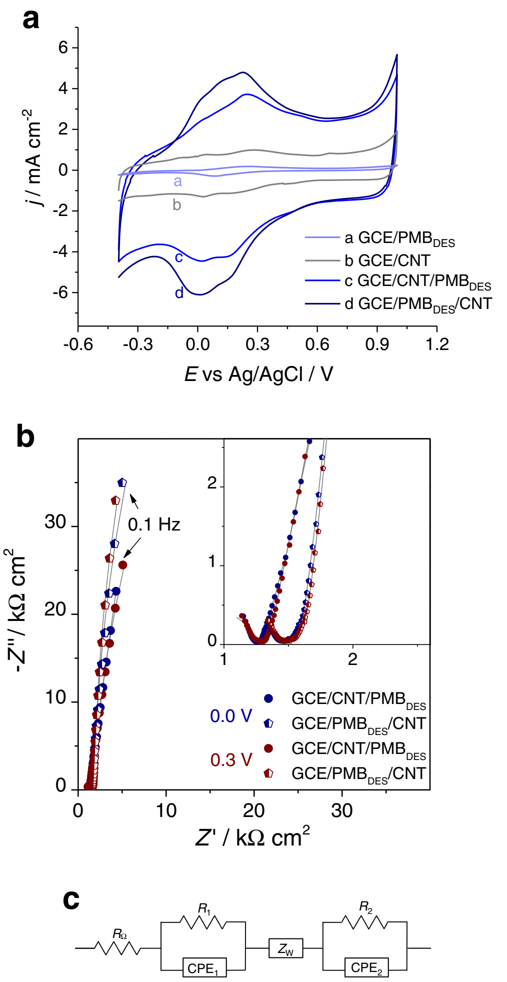

Fig. 2 **(a)** CVs recorded at GCE modified with either PMB_{DES} or CNT, or both in different configurations; $v = 50$ mV s^{-1}, 0.1 M KCl + 5 mM HCl; **(b)** Complex plane impedance spectra recorded in the frequency range 65 kHz - 0.1 Hz in 0.1 M KCl + 5 mM HCl at GCE/CNT/PMB_{DES} and GCE/PMB_{DES}/CNT at 0.0 and +0.3 V *vs.* Ag/AgCl; **(c)** equivalent electrical circuit used to fit the spectra

Analysis of the influence of scan rate, between 10 and 100 mV s^{-1} (results not shown), for the two PMB_{DES}-CNT hybrid film modified electrodes, reveals a diffusion-controlled electrochemical process, attributed to counter-ion diffusion through the composite film during PMB_{DES} oxidation and reduction.

Electrochemical impedance spectroscopy

Electrochemical impedance spectroscopy was carried out at GCE/CNT/PMB$_{DES}$ and GCE/PMB$_{DES}$/CNT at potentials between 0.0 and +0.3 V vs. Ag/AgCl, corresponding to the redox active region of the modified electrodes, as seen in the cyclic voltammograms in Fig. 2a. All spectra were similar, those at 0.0 and +0.3 V being presented in Fig. 2b, consisting of part of a semicircle in the high frequency region, attributed to charge transfer processes at the GCE surface, followed by a diffusive part in the medium frequency region and, finally, the beginning of a second semicircle of larger diameter at low frequency, correlated with the charge transport/separation in the CNT/PMB$_{DES}$ or PMB$_{DES}$/CNT film and at the film/electrolyte interface. Therefore, the equivalent circuit used to fit the spectra contained, besides the cell resistance, R_Ω, an R-CPE combination followed by a Warburg element and a second R-CPE (Fig. 2c). In the equivalent circuit, R_Ω is the uncompensated cell resistance, Z_W is the Warburg element, with $Z_W = R_W \mathrm{cth}[(\tau i\omega)^{\alpha}](\tau i\omega)^{-\alpha}$, where $\alpha < 0.5$, with R_W the diffusional resistance and τ the diffusional time constant, and the CPE are constant phase elements representing the charge separation of the double layer and the polarization of the polymer-CNT film, respectively, defined as $\mathrm{CPE} = [(Ci\omega)^{\alpha}]^{-1}$, modelled as a pure capacitor if $\alpha = 1$ or as a non-ideal capacitor, due to the porosity and non-homogeneity of the surface, for $0.5 < \alpha < 1$. The first CPE represents the charge separation at the electrode/polymer film interface while the second one comprises both the charge separation at the polymer/solution interface and the polarization of the polymer film.

The spectra can be compared with those recorded at electrodes modified with similar phenazine polymer-CNT structures, in which the polymer was synthesized from aqueous media [10, 11]. There are two main differences: i) the impedance values are lower and ii) the high frequency semicircle is considerably smaller in the present case, both indicating better electronic conductivity of the PMB$_{DES}$-CNT composites. In the case of GCE/PMB$_{DES}$, the spectra were different, the first R-CPE being extended over the high and mid-frequency region, and the lower part being fitted by a CPE, with lower α values [7], while in the case of GCE/CNT, the circuit was the same, excluding the element R_2.

Values of the circuit elements obtained by fitting the spectra are presented in Table S1. The values of R_1, CPE$_1$ and Z_W are similar at 0.0 and +0.3 V for both GCE/CNT/PMB$_{DES}$ and GCE/PMB$_{DES}$/CNT, the applied potential having a slightly greater influence on the R_2 and CPE$_2$ elements, reflecting the processes occurring inside the composite film and at the composite/electrolyte interface. Further analysis is given in the electronic supplementary information.

PMB$_{DES}$-CNT hybrid films in electrochemical detection

The electrochemical characterization of the PMB$_{DES}$-CNT-modified electrodes showed that the composites with both architectures, CNT/PMB$_{DES}$ and PMB$_{DES}$/CNT, greatly improve the overall electrochemical properties. The EIS studies revealed better electronic conductivity for GCE/PMB$_{DES}$/CNT. To further investigate which type of electrode design is better for electroanalytical purposes, GCE modified with both composites were used for the electrochemical detection of ascorbic acid (AA) and acetaminophen (APAP). Electrochemical measurements of AA were carried out using chronoamperometry, and square wave voltammetry (SWV) and differential pulse voltammetry (DPV) were used for APAP determinations, since the second analyte requires a higher applied potential for its detection. The results were compared with those of GCE/PMB$_{DES}$ and GCE/PMB$_{DES}$/CNT.

Determination of ascorbic acid

Chronoamperometric measurements were made at a fixed potential of +0.2 V vs. Ag/AgCl in 0.1 M KCl for AA using the different modified electrode sensors (Fig. 3a). The applied

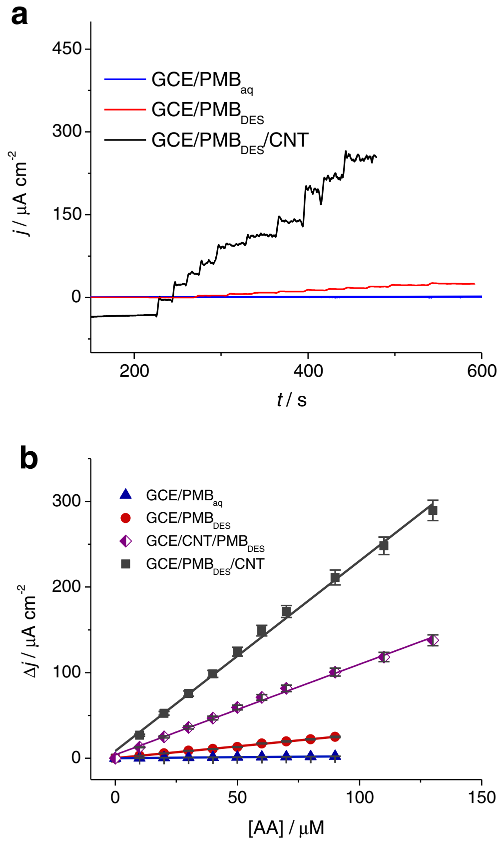

Fig. 3 Chronoamperometric determination of AA in 0.1 M KCl at +0.2 V *vs.* Ag/AgCl: (**a**) Fixed potential response and (**b**) corresponding calibration plots

potential in the chronoamperometric studies was chosen taking into account previous work on sensors for AA [1]. The analytical parameters of the CNT/PMB$_{DES}$ modified electrodes were determined from the corresponding calibration plots (Fig. 3b). The GCE/PMB$_{DES}$/CNT sensor had the lowest detection limit, LoD = 1.7 μM with a sensitivity of 2205 μA cm^{-2} mM^{-1} (RSD = 4.1%), whereas GCE/PMB$_{DES}$ had a LoD of 4.4 μM with a sensitivity of 340 μA cm^{-2} mM^{-1} (RSD = 2.8%). The LoD of the sensor based on PMB synthesized in aqueous solution was higher at 7.7 μM with a much lower sensitivity of only 23 μA cm^{-2} mM^{-1} (RSD = 1.9%) [7].

It was interesting to see that when CNT were deposited prior to polymer formation, the sensor had half the sensitivity of GCE/PMB$_{DES}$/CNT. This is probably related to the more compact, less porous, structure of this hybrid film, which hinders the diffusion of the analyte and thence reduces the active area. Similar tendencies were previously observed for other hybrid film sensors based on polymers and CNT [12, 13].

The analytical parameters of the sensors with different architectures revealed first the superior performance of PMB$_{DES}$ compared to PMB$_{aq}$, and, secondly, the better performance of hybrid films based on PMB$_{DES}$ and CNT, with the best being with CNT covering the polymer.

A comparison of some analytical parameters of GCE/PMB$_{DES}$/CNT with other polymer-based sensors found in the literature for ascorbate detection is made in Table 1 [5, 14–22]. As can be seen, only the sensor based on GCE/CNT/RuOHCF exhibited higher sensitivity, and that based on graphene ceramic nanofibres (GCE/ANF-C700) having lower but comparable sensitivity. Lower detection limits were found for only three other sensors, which makes GCE/PMB$_{DES}$/CNT a very promising tool for further applications.

Determination of acetaminophen

The anodic oxidation peak of APAP at GCE/PMB$_{DES}$ was measured by SWV (50 Hz frequency, 50 mV amplitude, 25 mV s^{-1} scan rate, 0.5 mV step potential) and DPV (50 mV amplitude, 4 mV s^{-1} scan rate, 2 mV step potential), see Fig. 4. In 0.1 M KCl electrolyte the anodic peak appears at around +0.67 V vs. Ag/AgCl in both DPV and SWV measurements. A linear response was observed up to 500 μM, and the relationship between the peak current and APAP concentration is expressed by the equations: Δj (μA cm^{-2}) = −15 (μA cm^{-2}) + 236*[APAP] (mM); $R^2 = 0.9993$, for the DPV method and Δj (μA cm^{-2}) = −6 (μA cm^{-2}) + 157*[APAP] (mM); $R^2 = 0.9994$ for the SWV method. The limit of detection, calculated on the basis of the 3*standard deviation ratio of sensitivity [23], was 1.6 μM APAP by DPV and 13.8 μM by SWV. Since the best analytical parameters were obtained by using DPV, it was chosen for evaluating the sensors with hybrid films of CNT and PMB$_{DES}$, as well as just CNT.

Typical calibration plots for the sensors with the different architectures are presented in Fig. 4c. For APAP concentrations up to 0.1 mM, the GCE/PMB$_{DES}$ sensor had a sensitivity of 0.360 μA cm^{-2} μM^{-1} (RSD 0.5%, $n = 5$) above which the response began to tail off, which can be attributed to adsorption on the modified electrode surface. GCE/PMB$_{DES}$/CNT

Table 1 Analytical parameters of AA sensors, based on similar modified electrodes, in the literature

Sensor architecture	Sensitivity / μA cm^{-2} mM^{-1}	LoD / μM	Reference
GCE/PMB$_{aq}$/PEDOT	46	13	[5]
GCE/NG/PEDOT	111	4.3	[14]
GCE/PEDOT/NG	103	5.6	[14]
GCE/NG/PNR	69	7.8	[14]
GCE/PNR/NG	113	5.2	[14]
GCE/CNT	384	4.3	[15]
GCE/CNT/PNR	375	4.7	[15]
GCE/CNT/RuOHCF	$132 \cdot 10^3$	0.09	[16]
GCE/PNB/CNT	857	2.4	[17]
SPE/PA/DS/CNT	105.3	-	[18]
GCE/hnpPt-Cu	120.7	25.1	[19]
GCE/Ni-CoHCF_G	-	0.15	[20]
GCE/ANF-C300	308	8.6	[21]
GCE/ANF-C700	$1.1 \cdot 10^3$	0.12	
GCE/RGO_Im	85	10	[22]
GCE/PMB$_{DES}$/CNT	$2.2 \cdot 10^3$	1.7	This work

NG nitrogen doped graphene, *PEDOT* poly(3,4-ethylenedioxythiophene), *PNR* poly(neutral red), *RuOHCF* ruthenium oxide hexacyanoferrate, *PA/DS* poly(allylamine) and dodecyl sulfate, *PNB* poly(Nile blue), *hnpPt-Cu* hierarchical nanoporous Pt-Cu alloy, *Ni-CoHCF_G* nickel-cobalt hexacyanoferrate microparticles deposited on graphene, *ANF-C300/700* alumina nanofibers modified by graphene foliates, *RGO_Im* electroreduced graphene oxide and imidazolium groups

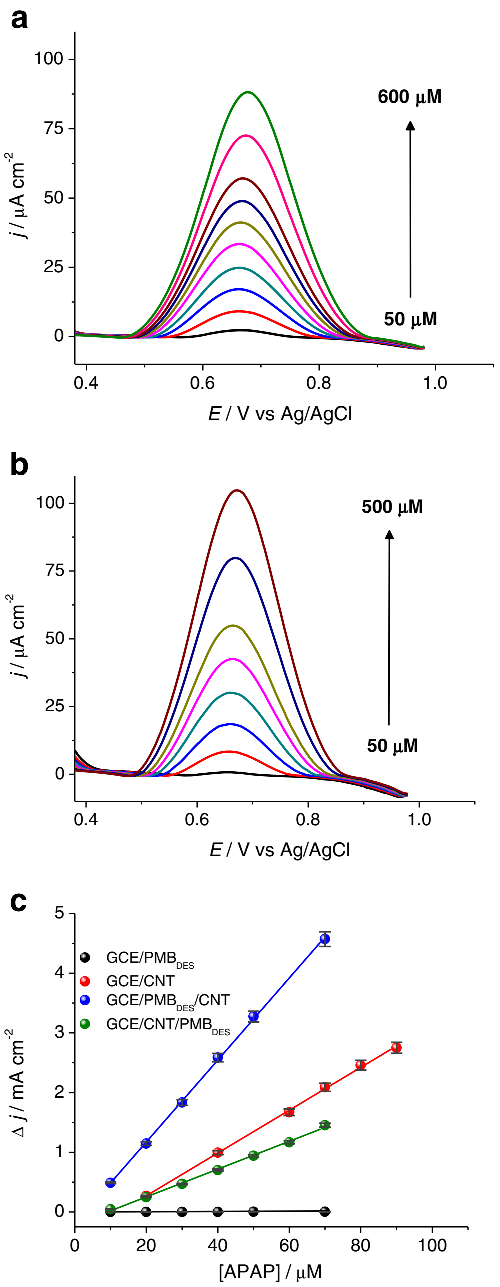

Fig. 4 **(a)** SWV ($v = 25$ mV s^{-1}) and (**b**) DPV ($v = 4$ mV s^{-1}) of APAP at GCE/PMB$_{DES}$ in 0.1 M KCl (step potential 2 mV, pulse amplitude 50 mV); (**c**) calibration plots from DPV

had a sensitivity approximatively three times higher than that of GCE/CNT/PMB$_{DES}$, of 68.6 µA cm^{-2} µM^{-1} (RSD 2.7%, n = 5) compared to 23.3 (RSD 2.3%, n = 5), as would be expected considering the performance of these two sensors for AA, where the hybrid with CNT covering the polymer also had superior sensitivity. As observed, the presence of CNT in the hybrid film leads to a substantial increase in sensitivity. The lowest detection limit, 1.6 µM, was also found for the GCE/PMB$_{DES}$/CNT electrode.

The repeatability of the analytical method employing the APAP sensors was examined by constructing a 5-point calibration plot 5 times, giving relative standard deviations of 2.7% for GCE/PMB$_{DES}$/CNT, 2.3% for GCE/CNT/PMB$_{DES}$, 1.4% for GCE/CNT and 0.5% for GCE/PMB$_{DES}$, respectively. The reproducibility of the sensors was also evaluated from 5-point calibration plots at three different electrodes, and RSD values were below 5% in all cases.

The GCE/PMB$_{DES}$/CNT sensor showed very good operational and storage stability, maintaining 94% of the initial response after 30 consecutive measurements of 50 µM APAP, and 98% after 1 month of storage in 0.1 M KCl at 4 °C. Long-term operational stability was assessed by measuring the sensor response to 50 µM APAP during one month. All electrodes were stored in 0.1 M KCl at 4 °C when not in use. The results exhibited only a very small decrease in sensitivity in the first 10 days and a slight decrease to about 90% of the initial sensitivity after one month. This demonstrates that the sensor possesses good stability and can be employed for practical applications. The stability of the sensors can be attributed to the excellent compatibility of the CNTs with the polymer network.

Table 2 compares the sensitivity and LoD of a number of sensors reported for APAP [10, 24–32]. As can be seen, the lowest LoD of 2.2 nM is achieved by a Pd/graphene oxide nanocomposite sensor, whereas the sensors in the present work exhibit the highest sensitivity for acetaminophen detection, considerably outclassing the other sensors.

The results confirm the greatly-enhanced analytical performance of the sensors related to the use of carbon nanotubes and of deep eutectic solvents for developing 3D network matrices with potential use in electroanalysis.

Determination of AA and APAP in pharmaceutical formulations

The sensor with the best analytical performance, GCE/PMB$_{DES}$/CNT was used for the detection of ascorbic acid and acetaminophen in pharmaceutical products: Aspirin Plus C®, FaringoHotDrink®, Paramolan C®, Coldrex Max Grip®, Theraflu®. Fixed potential amperometry at +0.2 V vs Ag/AgCl was used for AA determination and DPV for APAP determination, both in 0.1 M KCl at room temperature. The results of determinations using the standard addition method are displayed in Table S2.

For AA determination, the recovery factors were very close to 100%, showing that there were no significant interferences from the other compounds present in the formulation, which probably require a more positive potential than +0.2 V to be oxidized.

In the case of APAP, for all investigated pharmaceuticals, the oxidation potential of APAP was found at about the same value of E = + 0.67 V vs. Ag/AgCl as in the case of the standard. Analysis of the DPVs shows that there are several

Table 2 Analytical parameters of APAP sensors, based on similar electrode modifiers, in the literature

Sensor architecture	Sensitivity / μA cm^{-2} $μM^{-1}$	LoD / μM	Reference
CE/CNT/PMG	3.6	4.30	[10]
GCE/{CNT/ED}$_n$	2.3	0.09	[24]
GCE/PEI/CNT/HRP	0.3	1.36	[25]
Au/PANI-CNT/*Basillus sp.*/GA	24.6	2.90	[26]
GCE/poly[CoII-S]	1.0	0.30	[27]
CCE/CNT	3.3	0.12	[28]
GCE/poly-Trypan Blue	0.3	0.10	[29]
SPE/NHS-GO	0.63	0.17	[30]
GCE/GO/Pd	20.5	0.002	[31]
SPE/ProteinG MB/Ab	$9.6 \cdot 10^{-3}$	1.76	[32]
GCE/CNT/PMB$_{DES}$	23.3	3.11	This work
GCE/PMB$_{DES}$/CNT	68.7	1.64	This work

{CNT/ED}$_n$ layer by layers of ethylenediamine and CNT, *PEI/CNT/HRP* horseradish peroxidase entrapped into PEI doped with CNT, *PANI* polyaniline, *GA* glutaraldehyde, poly[CoII-S] N,N′- bis(salicylidene)ethylenediamine, *CCE* carbon–ceramic electrode, *NHS-GO* N-hydroxysuccinimide functionalized graphene oxide, *CE* composite electrode, *PMG* poly(methylene green), *GO* graphene oxide, *MB* magnetic beads, *Ab* antibody

*Geometric area not specified

components with redox properties, but with oxidation potentials sufficiently different from that of acetaminophen to enable accurate APAP determination, with very good recovery factors close to 100%. The results are in agreement with those reported by the manufacturer, indicating that there are no significant matrix interferences.

Conclusions

Two new hybrid composites based on the redox polymer PMB synthesized in DES medium and on CNT were evaluated for sensing applications. The poly(methylene blue) films electropolymerised in DES enhanced the CNT-modified GCE electrochemical properties, and enabled the construction of electrochemical sensors with superior analytical performances. The optimum sensor architecture was GCE/PMB$_{DES}$/CNT, which showed enhanced currents and a favourable electrocatalytic response. The applicability of the sensor was demonstrated using ascorbic acid and acetaminophen as analytes of interest. Low detection limits of 13.8 μM and 1.6 μM were obtained, with excellent sensitivities of 2.2 μA cm^{-2} $μM^{-1}$, and 68.7 μA cm^{-2} $μM^{-1}$, for ascorbic acid and acetaminophen, respectively, outclassing other similar sensors found in the literature. The new sensors showed good stability, reproducibility, repeatability and high recovery factors when used in pharmaceutical formulations, providing a new method for fast and highly sensitive detection of key analytes in complex matrices and broadening the use of green solvents in electrochemical sensors and pharmaceutical analysis.

Acknowledgements The authors are grateful for financial support from the Romanian National Authority for Scientific Research, CNCS - UEFISCDI, project number PNII-RU-TE-2014-4-0460 and from the Fundação para a Ciência e a Tecnologia (FCT), Portugal projects PTDC/QEQ-QAN/2201/2014, in the framework of Project 3599-PPCDT, and UID/EMS/00285/2013 (both co-financed by the European Community Fund FEDER), for financial support. O.H. thanks UMF for the internal grant number 7690/56/15.04.2016. M.M.B. thanks FCT for a postdoctoral fellowship SFRH/BPD/72656/2010.

Compliance with ethical standards The author(s) declare that they have no competing interests.

References

1. Barsan MM, Ghica ME, Brett CMA (2015) Electrochemical sensors and biosensors based on redox polymer/carbon nanotube modified electrodes: a review. Anal Chim Acta 881:1–23. doi:10.1016/j.aca.2015.02.059
2. Prathish KP, Carvalho RC, Brett CMA (2016) Electrochemical characterisation of poly(3,4-ethylenedioxythiophene) film modified glassy carbon electrodes prepared in deep eutectic solvents for simultaneous sensing of biomarkers. Electrochim Acta 187: 704–713. doi:10.1016/j.electacta.2015.11.092
3. Wagle DV, Zhao H, Baker GA (2014) Deep eutectic solvents: sustainable media for nanoscale and functional materials. Acc Chem Res 47:2299–2308. doi:10.1021/ar5000488
4. Pauliukaite R, Ghica ME, Barsan MM, Brett CMA (2010) Phenazines and Polyphenazines in electrochemical sensors and biosensors. Anal Lett 43:1588–1608. doi:10.1080/00032711003653791
5. Kakhki S, Barsan MM, Shams E, Brett CMA (2013) New robust redox and conducting polymer modified electrodes for ascorbate sensing and glucose biosensing. Electroanalysis 25:77–84. doi:10.1002/elan.201200402

6. Kakhki S, Barsan MM, Shams E, Brett CMA (2013) New redox and conducting polymer modified electrodes for cholesterol biosensing. Anal Methods 5:1199–1204. doi:10.1039/c3ay26409b
7. Hosu O, Barsan MM, Cristea C et al (2017) Nanostructured electropolymerized poly(methylene blue) films from deep eutectic solvents. Optimization and characterization Electrochim Acta 232: 285–295. doi:10.1016/j.electacta.2017.02.142
8. Chen Q, Espey MG, Krishna MC et al (2005) Pharmacologic ascorbic acid concentrations selectively kill cancer cells: action as a prodrug to deliver hydrogen peroxide to tissues. Proc Natl Acad Sci U S A 102:13604–13609. doi:10.1073/pnas.0506390102
9. Cernat A, Tertiş M, Săndulescu R et al (2015) Electrochemical sensors based on carbon nanomaterials for acetaminophen detection: a review. Anal Chim Acta 886:16–28. doi:10.1016/j.aca.2015.05.044
10. Barsan MM, Toledo CT, Brett CMA (2015) New electrode architectures based on poly(methylene green) and functionalized carbon nanotubes: characterization and application to detection of acetaminophen and pyridoxine. J Electroanal Chem 736:8–15. doi:10.1016/j.jelechem.2014.10.026
11. Pifferi V, Barsan MM, Ghica ME et al (2013) Synthesis, characterization and influence of poly(brilliant green) on the performance of different electrode architectures based on carbon nanotubes and poly(3,4-ethylenedioxythiophene). Electrochim Acta 98:199–207. doi:10.1016/j.electacta.2013.03.048
12. Braik M, Barsan MM, Dridi C et al (2016) Highly sensitive amperometric enzyme biosensor for detection of superoxide based on conducting polymer/CNT modified electrodes and superoxide dismutase. Sensors Actuators B Chem 236:574–582. doi:10.1016/j.snb.2016.06.032
13. Barsan MM, Pifferi V, Falciola L, Brett CMA (2016) New CNT/poly(brilliant green) and CNT/poly(3,4-ethylenedioxythiophene) based electrochemical enzyme biosensors. Anal Chim Acta 927: 35–45. doi:10.1016/j.aca.2016.04.049
14. Barsan MM, Prathish KP, Sun X, Brett CMA (2014) Nitrogen doped graphene and its derivatives as sensors and efficient direct electron transfer platform for enzyme biosensors. Sensors Actuators B Chem 203:579–587. doi:10.1016/j.snb.2014.07.019
15. Carvalho RC, Gouveia-Caridade C, Brett CMA (2010) Glassy carbon electrodes modified by multiwalled carbon nanotubes and poly(neutral red): a comparative study of different brands and application to electrocatalytic ascorbate determination. Anal Bioanal Chem 398:1675–1685. doi:10.1007/s00216-010-3966-3
16. Raoof JB, Ojani R, Baghayeri M et al (2011) A selective sensor based on a glassy carbon electrode modified with carbon nanotubes and ruthenium oxide/hexacyanoferrate film for simultaneous determination of ascorbic acid, epinephrine and uric acid. Anal Methods 3:2367–2373. doi:10.1039/c1ay05305a
17. Kul D, Ghica ME, Pauliukaite R, Brett CMA (2013) Talanta a novel amperometric sensor for ascorbic acid based on poly (Nile blue a) and functionalised multi-walled carbon nanotube modified electrodes. Talanta 111:76–84. doi:10.1016/j.talanta.2013.02.043
18. Cortez ML, Ceolin M, Azzaroni O, Battaglini F (2011) Electrochemical sensing platform based on polyelectrolyte-surfactant supramolecular assemblies incorporating carbon nanotubes. Anal Chem 83:8011–8018. doi:10.1021/ac202213t
19. Zhao D, Fan D, Wang J, Xu C (2015) Hierarchical nanoporous platinum-copper alloy for simultaneous electrochemical determination of ascorbic acid, dopamine, and uric acid. Microchim Acta 182:1345–1352. doi:10.1007/s00604-015-1450-7
20. Wang Q, Tang QL (2014) Improved sensing of dopamine and ascorbic acid using a glassy carbon electrode modified with electrochemically synthesized nickel-cobalt hexacyanoferrate microparticles deposited on graphene. Microchim Acta 182:671–677. doi:10.1007/s00604-014-1371-x
21. Taleb M, Ivanov R, Bereznev S et al (2017) Graphene-ceramic hybrid nanofibers for ultrasensitive electrochemical determination of ascorbic acid. Microchim Acta 184:897–905. doi:10.1007/s00604-017-2085-7
22. Wu F, Huang T, Hu Y et al (2016) Differential pulse voltammetric simultaneous determination of ascorbic acid, dopamine and uric acid on a glassy carbon electrode modified with electroreduced graphene oxide and imidazolium groups. Microchim Acta 183: 2539–2546. doi:10.1007/s00604-016-1895-3
23. Brett CMA, Oliveira Brett AM (1998) Electroanalysis. Oxford University Press, New York
24. Li Y, Feng S, Li S et al (2014) A high effect polymer-free covalent layer by layer self-assemble carboxylated MWCNTs films modified GCE for the detection of paracetamol. Sensors Actuators B Chem 190:999–1005. doi:10.1016/j.snb.2013.09.052
25. Tertis M, Florea A, Sandulescu R, Cristea C (2013) Carbon based electrodes modified with horseradish peroxidase immobilized in conducting polymers for acetaminophen analysis. Sensors (Basel) 13:4841–4854. doi:10.3390/s130404841
26. Bayram E, Akyilmaz E (2016) Development of a new microbial biosensor based on conductive polymer/multiwalled carbon nanotube and its application to paracetamol determination. Sensors Actuators B Chem 233:409–418. doi:10.1016/j.snb.2016.04.029
27. Sonkar PK, Ganesan V, Prajapati A (2016) Polymeric co(salen) scaffold for the electrochemical determination of acetaminophen in pharmaceutical sample. Ionics (Kiel) 22:1741–1749. doi:10.1007/s11581-016-1699-9
28. Habibi B, Jahanbakhshi M, Pournaghi-Azar MH (2011) Simultaneous determination of acetaminophen and dopamine using SWCNT modified carbon-ceramic electrode by differential pulse voltammetry. Electrochim Acta 56:2888–2894. doi:10.1016/j.electacta.2010.12.079
29. Taei M, Jamshidi MS (2017) A voltammetric sensor for simultaneous determination of ascorbic acid, noradrenaline, acetaminophen and tryptophan. Microchem J 130:108–115. doi:10.1016/j.microc.2016.08.011
30. Tertiş M, Hosu O, Fritea L et al (2015) A novel label-free Immunosensor based on activated graphene oxide for acetaminophen detection. Electroanalysis 27:638–647. doi:10.1002/elan.201400583
31. Li J, Liu J, Tan G et al (2014) High-sensitivity paracetamol sensor based on Pd/graphene oxide nanocomposite as an enhanced electrochemical sensing platform. Biosens Bioelectron 54:468–475. doi:10.1016/j.bios.2013.11.001
32. Hosu O, Tertiş M, Săndulescu R, Cristea C (2015) Protein G magnetic beads based immunosensor for sensitive detection of acetaminophen. Farmacia 63:140–145